Chemical Engineering Journal 464 (2023) 142557

Contents lists available at ScienceDirect

Chemical Engineering Journal

journal homepage: www.elsevier.com/locate/cej

Behavior and fate of short chain chlorinated paraffins (SCCPs) in different oxidation reactions

Quanyun Ye [a,b,1], Qingmei Song [a,b,1], Jingyan Zhou [a,b], Yingxin Wu [a,b,*], Yue Zhou [a,b], Jie Zhang [a,b], Wencheng Wu [a,b,*]

[a] South China Institute of Environmental Sciences, Ministry of Ecology and Environment, Guangzhou 510655, China
[b] Guangdong Engineering & Technology Research Center for System Control of Livestock and Poultry Breeding Pollution, Guangzhou 510655, China

ARTICLE INFO

Keywords:
Short-chain chlorinated paraffins
Advanced oxidation
Soil remediation
Density functional theory

ABSTRACT

Short chain chlorinated paraffins (SCCPs) have attracted extensive attention due to their adverse effects on soil organisms and humans. However, comprehensive understanding of the degradation of SCCPs is still limited. In this work, the behavior and fate of SCCPs during advanced oxidation processes (AOPs) in contaminated soil were studied. The concentration and congener profile of SCCPs before and after the oxidations were determined. Results showed that SCCPs (1 mg kg^{-1}) could be effectively degraded within 120 h by four common oxidants, including hydrogen peroxide (H_2O_2), Fenton (H_2O_2/Fe^{2+}), potassium permanganate ($KMnO_4$), and sodium persulfate ($Na_2S_2O_8$). The optimal degradation efficiency followed the order $KMnO_4$ (93.3 %) > $Na_2S_2O_8$ (91.9 %) > Fenton (90.4 %) > H_2O_2 (84.3 %). After the oxidation treatment, the relative abundance of $C_{10}Cl_{8\sim10}$, $C_{11}Cl_{8\sim10}$, $C_{12}Cl_{8\sim10}$, and $C_{13}Cl_{8\sim10}$ increased, among that $C_{10}H_{13}Cl_9$ increased the most (1.71 % − 2.52 %, in mass ratio). While the relative abundance of $C_{10}Cl_{5\sim7}$, $C_{11}Cl_{5\sim7}$, and $C_{12}Cl_{6\sim7}$ decreased significantly, and $C_{11}H_{18}Cl_6$ decreased the most (−3.81 % − −6.18 %, in mass ratio). Density functional theory (DFT) calculations were used to explain these observations. Compared to carbon atomic percentage, chlorine atomic percentage had greater impacts on the degradation of SCCP congeners, which showed a significant negative correlation. However, four congeners consistently failed to follow this pattern, such as $C_{12}H_{21}Cl_5$, $C_{13}H_{22}Cl_6$, $C_{12}H_{16}Cl_{10}$, and $C_{13}H_{18}Cl_{10}$. This work is expected to provide data and technical support for remediation in typical SCCPs contaminated soil.

1. Introduction

Chlorinated paraffins (CPs) are a complex mixture of polychlorinated *n*-alkanes with general molecular formula $C_nH_{(2n+2)-m}Cl_m$ (n = 10 ~ 30, m = 1 ~ 17) [1,2]. CPs homologues are very complex in composition due to the differences in carbon chain length, chlorination degree, and chlorine bond position, which are subdivided into short-chain chlorinated paraffins (SCCPs, $C_{10\sim13}$), medium-chain chlorinated paraffins (MCCPs, $C_{14\sim17}$) and long-chain chlorinated paraffins (LCCPs, $C_{18\sim30}$) according to the length of carbon chain [3]. The physicochemical properties of CPs vary widely, mainly related to the carbon chain length and chlorination degree, among which SCCPs have the advantages of low volatility, flame retardancy, good electrical insulation, and low price, often in use for a wide range of industrial applications, such as flame retardants, plasticizers, sealants, paints, and lubricant products [4–6]. SCCPs are also of greatest concern, in 2017, SCCPs were classified as the persistent organic pollutants (POPs) in the Stockholm Convention and would be banned or strictly restricted worldwide [7]. However, as the largest producer and consumer of CPs, China has just started to impose only few restrictions on SCCPs recently [8,9], and limited data for environmental behavior and fate of SCCPs are available due to the highly complex compositions of SCCPs and their difficult quantification.

SCCPs have a high annual output and are used in almost all industries, which are inevitably released into the environment during production, storage, transportation and use [10,11]. As a result, the presence of SCCPs in the environment has been detected in various environmental media, such as air, water, sediment, soil, biota, and human body worldwide [12]. The environmental behavior characteristics of SCCPs mainly include environmental persistence [13], long-distance transport [14], bioaccumulation [15], and toxicity [16].

* Corresponding authors at: South China Institute of Environmental Sciences, Ministry of Ecology and Environment, Guangzhou 510655, China.
E-mail addresses: wuyingxin@scies.org (Y. Wu), wuwencheng@scies.org (W. Wu).
[1] Quanyun Ye and Qingmei Song are co-first authors of the article.

https://doi.org/10.1016/j.cej.2023.142557
Received 15 November 2022; Received in revised form 17 March 2023; Accepted 20 March 2023
Available online 22 March 2023

SCCPs pollution has become a global threat, attracting extensive attention. Researches showed that the toxicity mechanism of SCCPs was mainly related to oxidative stress, metabolic disorders, and endocrine disorders, which had great toxicity to organisms, including developmental toxicity, carcinogenicity, and immune regulation disorders, etc [16]. SCCPs were also toxic to mammals and could cause damage to their liver, kidney, thyroid and parathyroid glands [13]. We previously reported that the composition and structure of the soil bacterial community were significantly affected by SCCPs even in low contents [17]. At present, SCCPs are very common in soil with complex behaviors, which have great adverse effects on soil organisms and humans. Thus, the remediation of SCCPs-contaminated soil is urgently needed.

Compared with other common POPs [18,19], there are few literature reports available at present on the degradation of SCCPs and it is hard to directly compare the observations from different authors, since reaction kinetics, intermediates, and transformation pathways may differ significantly, depending on the degradation method employed. Advanced oxidation processes (AOPs) primarily decompose target pollutants by generating highly active radicals, such as hydroxyl radical (•OH), superoxide radical ($O_2•^-$), and sulfate radical anion ($SO_4•^-$), which can effectively degrade refractory compounds and generate small molecular substances with high efficiency [20–22]. The most common AOPs in site restoration mainly include hydrogen peroxide (H_2O_2) oxidation, Fenton (H_2O_2/Fe^{2+}) method, persulfate ($Na_2S_2O_8$) activation, potassium permanganate ($KMnO_4$) oxidation, etc, which are very different in oxidation mechanisms [23]. AOPs have a broad application prospect in the degradation of SCCPs and remediation contaminated soil. It is very essential to understand the behavior and removal of SCCPs in different AOPs in order to reduce their ecological risks and potential negative impacts on the contaminated site. However, complex effects of both atomic ratio and homologues composition of SCCPs on AOPs remain poorly understood.

In the present study, we carried out a detailed analysis of SCCPs oxidation response behavior with common different oxidants (H_2O_2, Fenton, $KMnO_4$, and $Na_2S_2O_8$), and the key factors affecting the fate and transport of SCCPs during oxidation process. The degradation effects of different oxidants were compared, and the abundance changes of SCCP homologue patterns were analyzed. Moreover, density functional theory (DFT) calculations were used to explore the active site of SCCPs and the degradation mechanism. The results of this study are expected to gain insights into the behavior and fate of SCCPs in different oxidations, which can provide a certain theoretical basis and technical support for the remediation of SCCPs contaminated soil.

2. Materials and methods

2.1. Materials

Standard mixtures of SCCPs (51.5 % Cl, 55.5 % Cl, and 63 % Cl) and ε-hexachlorocyclohexane (ε-HCH) were purchased from Dr. Ehrenstorfer GmbH (Germany). $^{13}C_{10}$-*trans*-chlordane, dichloromethane (DCM), and *n*-hexane (HEX) were purchased from Cambridge Isotop Laboratory Inc. (USA). Sodium sulfate (Na_2SO_4), hydrogen peroxide (H_2O_2), ferrous sulfate ($FeSO_4·7H_2O$), potassium permanganate ($KMnO_4$), and sodium supersulphate ($Na_2S_2O_8$) were purchased from Anpel Chemical Reagent Co., ltd. (Shanghai, China). All the chemicals were analytical reagent (AR) and used without purification.

2.2. Preparation of SCCPs contaminated soil samples

A total of 2000 g test soil without SCCPs pollution was collected in Guangzhou, China and ground through a 10-mesh sieve prior to use. A 10 mg of industrial grade SCCPs reagent was diluted into 100 mL of hexane, and then 20 mL of this solution was added to 100 g of soil sample. The mixture was blended into the remaining 1900 g of soil for 30 days, during which time the mixture was stirred regularly. The contaminated soil samples were freeze-dried, passed through a 100-mesh sieve, and stored for later use.

2.3. Sample pretreatment for SCCPs determination

A soil sample (5.0 g) and 0.1 mL of $^{13}C_{10}$-*trans*-chlordane (100 μg mL^{-1}) were adding into the centrifuge tube prior to adding 20 mL of HEX-DCM mixed solutions for ultrasonic extraction at 50 °C for 30 min. The supernatant was then collected and two more 20 min ultrasonic extractions were performed at 50 °C (The dosage of HEX-DCM (1:1, *V/V*) was 15 mL each time). All collected supernatants were concentrated to 2 mL by using a rotary evaporator.

2.4. Characterizations

Instrumental analysis was performed using a high-resolution gas chromatograph coupled with electron capture negative ion-mass spectrometer (GC-ECNI-MS, GC-2010 Plus, Shimadzu). The chromatographic column was HP-5MS with a specification of 30 m × 0.25 mm × 0.25 μm. The carrier gas was high purity nitrogen (N_2, 99.999 %) at a flow rate of 4 mL min^{-1}. The temperature of detector and injector were set at 310 °C and 270 °C, respectively. The column heating program was set as follows: temperature increased to 150 °C at a rate of 20 °C min^{-1} after holding at 90 °C for 1 min, and then increased to 300 °C at a rate of 15 °C min^{-1} for 4 min. The GC-ECD results of different oxidation treatments were shown in the Supporting Information, Fig. S1.

2.5. Degradation experiments

The soil sample of 5.0 g was added in a 50 mL polytetrafluoroethylene centrifuge tube, and different kinds of oxidizing agents were added according to the dosage shown in Table 1. The water/soil ratio was set to 1:1.5 and the pH value was unadjusted unless otherwise stated. The concentration of SCCPs was tested after 120 h of reaction. The degradation efficiency (η) was obtained following Eq. (1):

$$\eta = (C_0 - C_t)/C_0 \times 100\% \quad (1)$$

C_0: Initial concentration of SCCPs, mg kg^{-1}, C_t: Concentration of SCCPs at reaction time t, mg kg^{-1}. All experiments were carried out in triplicate.

2.6. DFT calculations

Geometric optimization of SCCPs was performed by Gaussian 16 W at the B3LYP/6–31 g(*) level. The Fukui Function was used to analyze the vulnerable sites of SCCPs [24], which was widely used to predict the

Table 1
The dosage of different oxidants.

Sample	Oxidant	Concentration	Dosage (%)
CK	ultrapure water	/	/
H (1)	H_2O_2	30 %	2
H (2)	H_2O_2	(ρ = 1.112 g mL^{-1})	4
H (3)	H_2O_2		6
H (4)	H_2O_2		8
F (1)	Fenton	$m(H_2O_2):m(Fe^{2+})$ = 5:1	2
F (2)	Fenton		4
F (3)	Fenton		6
F (4)	Fenton		8
K (1)	$KMnO_4$	solid, AR	2
K (2)	$KMnO_4$		4
K (3)	$KMnO_4$		6
K (4)	$KMnO_4$		8
P (1)	$Na_2S_2O_8$	solid, AR	2
P (2)	$Na_2S_2O_8$		4
P (3)	$Na_2S_2O_8$		6
P (4)	$Na_2S_2O_8$		8

reaction sites of electrophilic, nucleophilic, and radical attack. The results of calculation were displayed on Visual Molecular Dynamics (VMD) based on the output file from Multiwfn 3.8 program [25–27]. More details about DFT calculations were described in the Supporting Information, Text S1.

3. Results and discussion

3.1. Degradation efficiency of SCCPs by different oxidants

The degradation efficiency of four different oxidants (H_2O_2(H), Fenton(F), $KMnO_4$(K), and $Na_2S_2O_8$(P)) at different concentrations (2 %, 4 %, 6 %, and 8 %) on SCCPs were presented in Fig. 1. Overall, ∑SCCPs decreased significantly along the four kinds of oxidants within 120 h, and the degradation efficiency under the optimal dosage conditions was in the order of $KMnO_4$ > $Na_2S_2O_8$ > Fenton > H_2O_2. Among them, the redox potential of $KMnO_4$ is relatively low (1.68 eV), but $KMnO_4$ can be applied without activation, which is highly influenced by pH and has the strongest oxidation capacity under acidic conditions [28]. The pH value of SCCPs-contaminated soil was about 4.5, which was conducive to the better oxidation effect of $KMnO_4$. Moreover, $KMnO_4$ shows selectivity for organic pollutants during oxidation, especially for those electron-rich groups, such as sulphide, aniline group, and organic chloride [29–31]. Therefore, $KMnO_4$ had an excellent degradation effect on SCCPs in this research. The oxidation effect of $Na_2S_2O_8$ on organic contaminated soil was mainly due to the following aspects [32–34]: (i) The peroxydisulfate anion ($S_2O_8^{2-}$) has relatively high oxidation potential (2.01 eV), can be directly react with some organic pollutants; (ii) Minerals (Fe, Mn, etc.) in soil can promote the bond breaking of persulfate and produce $SO_4\bullet^-$ (2.5–3.1 eV) and •OH, which can attack organic pollutants. Fenton process can produce certain •OH, which is more limited than $SO_4\bullet^-$, including lower redox potential (1.8–2.7 eV vs 2.5–3.1 eV) and shorter lifetime ($t_{1/2} = 10^{-3}$ μs vs 30–40 μs) [35,36]. Compared with the other three oxidants, the degradation efficiency of SCCPs was the lowest when using H_2O_2 alone. On the one hand, H_2O_2 shows the lowest oxidation potential (1.8 eV) and can be easily decomposed into H_2O and O_2, on the other hand, H_2O_2 is very inefficient at producing •OH, resulting in low degradation efficiency [37]. Equations of SCCPs degradation in different AOPs were described in the Supporting Information, Text S2.

Unexpectedly, the degradation efficiency of ∑SCCPs by the four oxidants did not always increase with the increasing added amount, and the optimal amount was different. The best degradation efficiency of SCCPs was achieved by adding 2 % of H_2O_2, Fenton, or $KMnO_4$, with a reduction of SCCPs concentration by 84.3 %, 90.4 %, and 93.3 % respectively. For $Na_2S_2O_8$, the optimal amount was 6 %, which degraded 91.9 % of SCCPs. It was noted that the degradation efficiency of ∑SCCPs decreased when the dosage of Fenton and $KMnO_4$ increased. Especially the degradation efficiency of ∑SCCPs by 8 % Fenton (52.7 %) was obviously lower than those by 2 % (90.4 %), which implied that those longer chain CPs in soil were likely to react with oxidant in the degradation process and generate SCCPs when the content of oxidant or oxidizing capacity was too high.

Among the four oxidants, $KMnO_4$ had the best degradation effect in the contaminated soil. However, the oxidation process would consume H^+ and produce OH^-, which significantly increased the soil pH (Table S1). In addition, soil permeability function would be affected when $KMnO_4$ was used in excessive quantities. $Na_2S_2O_8$ also showed a good degradation effect of SCCPs with a long service life in contaminated soil, but the dosage was relatively more than other oxidants, and would decrease the pH value. Fenton treatment would degrade longer chain CPs, which further generated shorter chain SCCPs, and also decreased the pH value of soil. In summary, the actual site restoration should comprehensively consider the types of pollutants, soil pH, amount of oxidant, price and other conditions to select the appropriate oxidation methods. These conclusions provided data support for the remediation of SCCPs in actual contaminated soil.

3.2. Analysis of SCCP homologues degraded by different oxidants

3.2.1. Distribution of SCCP homologues in contaminated soil

To determine the relative abundance variations of SCCP homologues and understand the oxidation behavior, SCCP homologue profiles categorized by carbon and chlorine atom groups at different oxidation treatments were plotted. The composition of SCCP homologues without oxidants was presented in Fig. 2. Of all the carbon chain groups, the SCCP homologue of C_{11} showed the highest abundance, and followed by C_{10}, C_{12}, and C_{13} homologues. In the chlorine homologue profile, the homologue with chlorine atom number of 6 had the highest relative content for C_{10}, and chlorine atom number of 7 had the highest relative content for $C_{11\sim13}$ congener groups. Chlorine atom number of 5 or 10 was the least in abundance for all soil samples.

Significant differences in SCCP homologue profiles were shown after four kinds of oxidation treatment, as presented in Fig. 3. The varied congener profiles in different samples also indicated the distinct oxidation behaviors of SCCP congeners. In the carbon homologue profile, the relative content of SCCPs with carbon atom number 11 decreased from 35 % to about 30 % ~ 32 %, however, it was still the

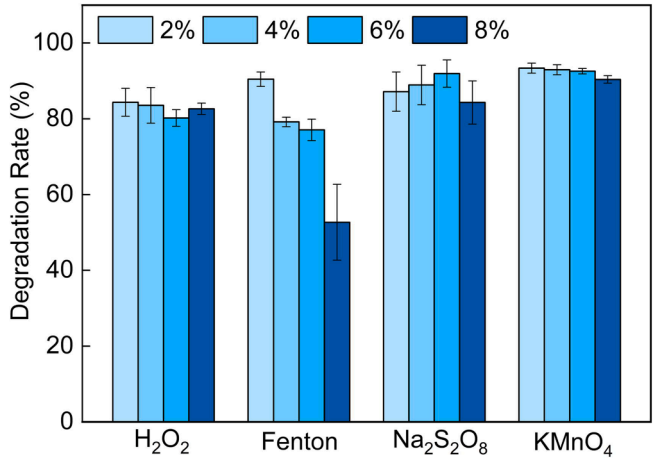

Fig. 1. Degradation efficiency of SCCPs by different oxidants. Reaction conditions: 5 g of SCCPs contaminated soil (1 mg kg^{-1}), the water/soil ratio 1:1.5, initial pH 4.5 and ambient temperature.

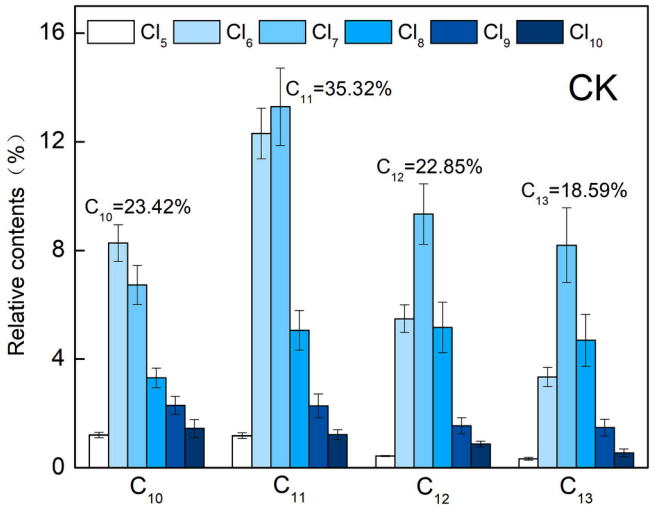

Fig. 2. Soil SCCP homologue profile without oxidation. Reaction conditions: the water/soil ratio 1:1.5, initial pH 4.5 and ambient temperature.

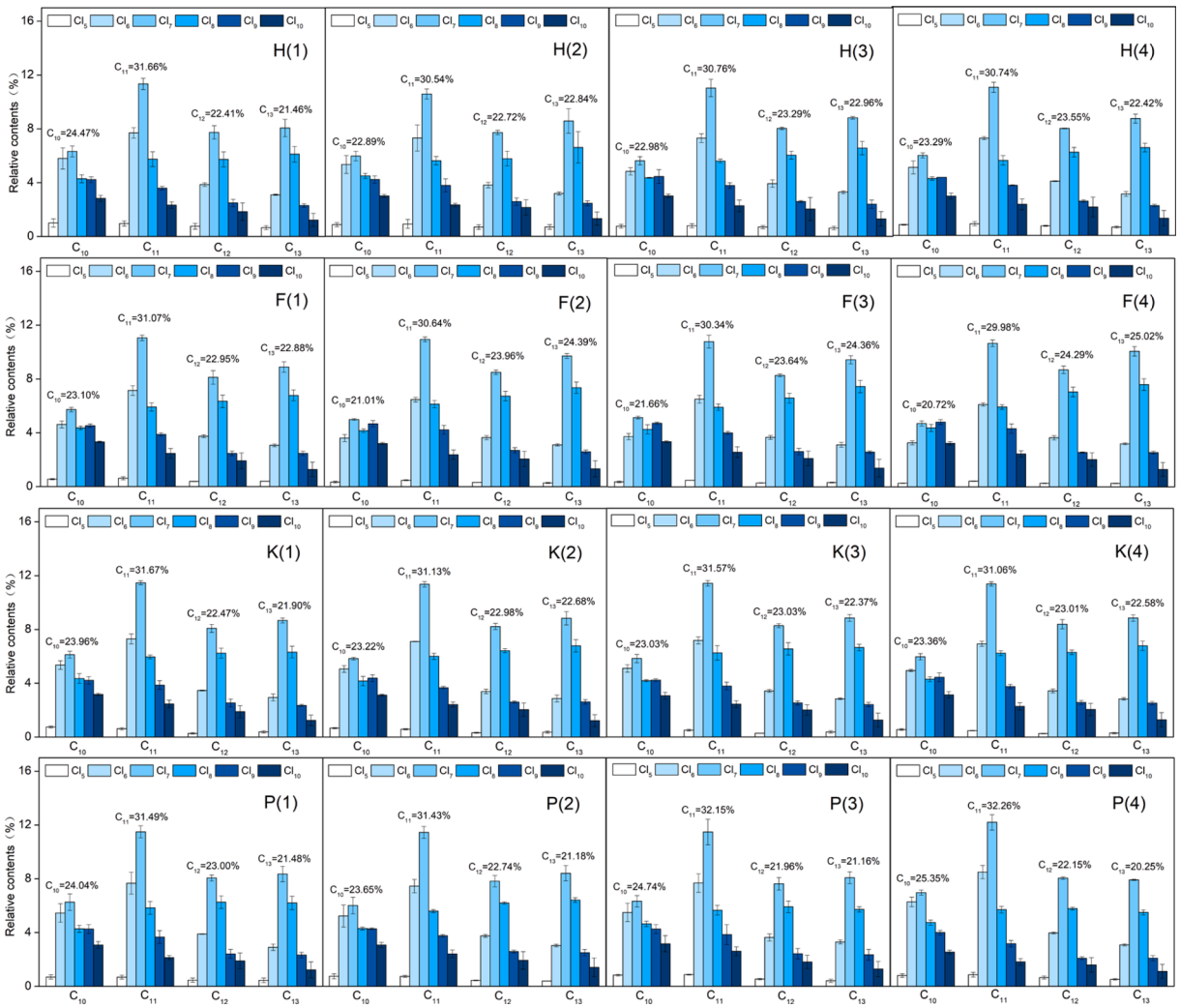

Fig. 3. Distribution of SCCP homologues after oxidation treatment. Reaction conditions: 5 g of SCCPs contaminated soil (1 mg kg^{-1}), the water/soil ratio 1:1.5, initial pH 4.5 and ambient temperature.

most predominant congeners in all soil samples. The reason was that C_{11} congeners were easily oxidative degraded into smaller molecules. Some long-chain SCCPs were also degraded to C_{11} congeners during the reaction, but this amount was lower, thus resulting in a decrease in the relative content of C_{11} congeners. Little discernible variation could be seen for C_{10} and C_{12} congeners after oxidation treatment, it was because the production and degradation of C_{10}/C_{12} congeners maintained a relatively dynamic balance. Interestingly, the relative content of C_{13} congeners was increased in all samples. On the one hand, C_{13} congeners of SCCPs were more difficult to be degraded. More importantly, it was judged that a small number of C_{13} congeners would be oxidized to shorter carbon chain SCCPs, while some long chain CPs were oxidized to C_{13} congeners. The production amount of C_{13} congeners was greater than the degradation amount, which led to the obvious increase of C_{13} congeners after the oxidation treatment. This conclusion was supported by the results of Fenton treatment, especially for F(4) treatment, where the degradation efficiency of SCCPs was the lowest and the relative content of C_{13} homologue profile was as high as 25.02 %.

3.2.2. Results of significance analysis

Statistical analysis of significance test between oxidant type, dosage, and degradation efficiency for SCCPs was conducted using 2-tailed paired *t*-test at a 5 % level of significance. As shown in Fig. 4(a), no significant discrepancy in abundance of SCCP homologue profiles was found by the same oxidant with different concentrations (2 % ~ 8 %) except for Fenton treatment, further proving that oxidant concentration had little effects on the abundance of SCCP homologue profiles. Fig. 4(b) showed that different types of oxidants led to significantly different abundances of SCCP homologues even with the same amount of additions, particularly with the amount of 8 %. Different kinds of oxidants showed different redox properties and different selectivity for SCCPs, further demonstrating the vital role of the oxidant type for the abundance of SCCP homologues.

3.2.3. Results of principal component analysis (PCA) analysis

The PCA plot for SCCP homologues distribution and different oxidation methods were presented in Fig. 5. The first two axes explained 85.2 % of the information about the abundance of SCCP homologues in different oxidation conditions. The results showed that control group (CK) and oxidation groups (F, H, K, P) were obviously divided into two clusters, indicating that there were significant differences in the SCCP homologues distribution before and after oxidation. In addition, different concentrations of H_2O_2 and $KMnO_4$ treatments did not significantly affect the abundance of SCCPs. However, for Fenton, the results of F1 deviated from those of F2, F3, and F4, indicating that the concentration had a certain influence on the SCCP homologues distribution. Similarly, for $Na_2S_2O_8$, the oxidant concentration also affected on the SCCP homologues distribution (see Fig. 6).

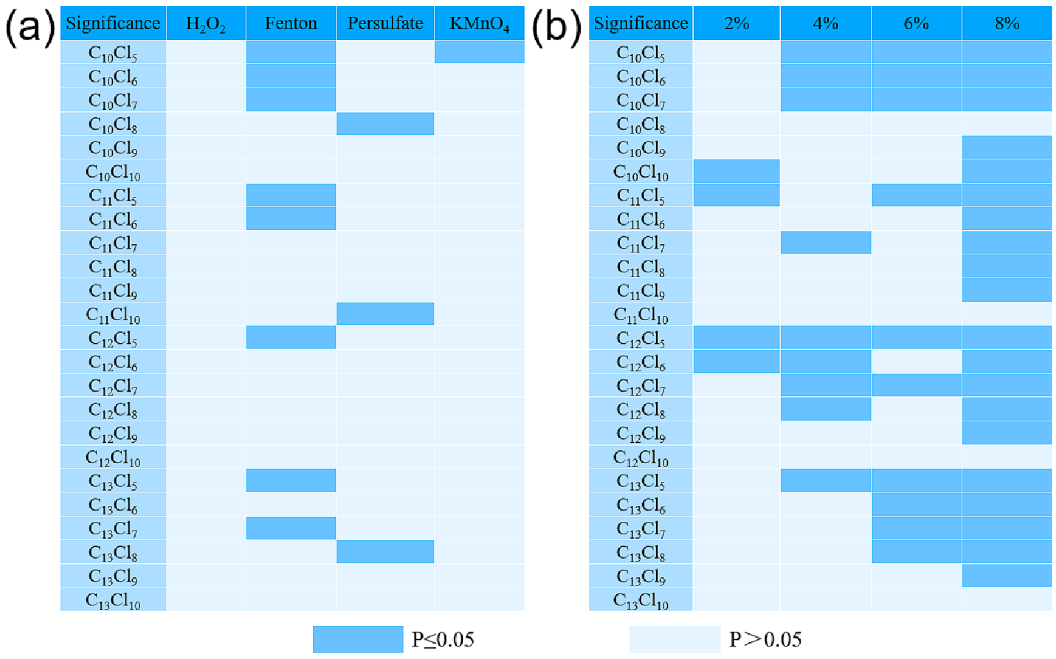

Fig. 4. Pearson correlation between the oxidation treatment parameter and relative abundance of congener distribution patterns. (a) The same oxidant with different concentrations (2 %~8%); (b) The same concentration with different types of oxidants.

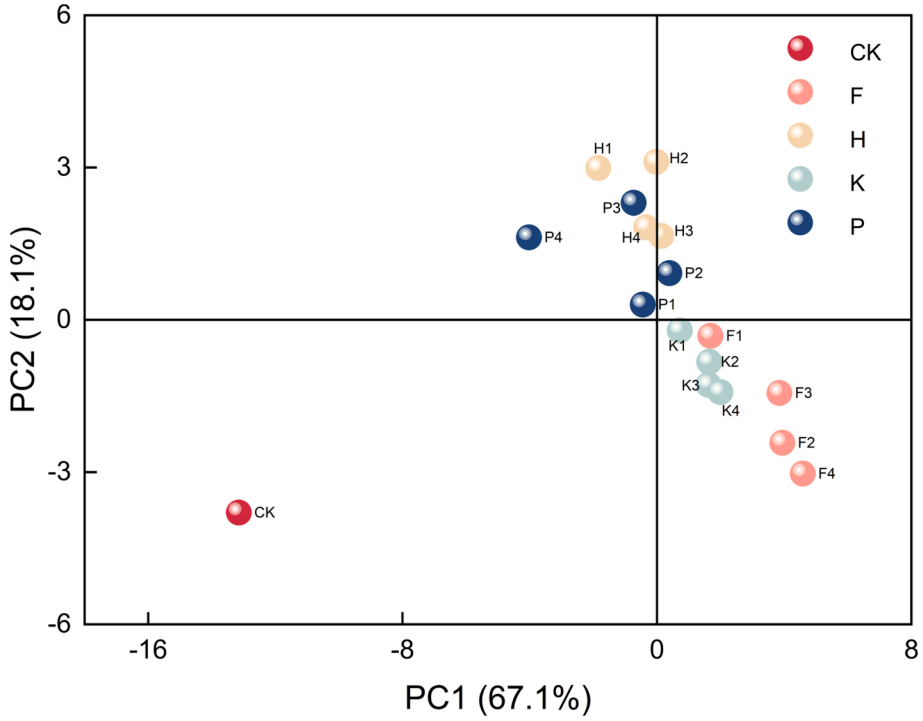

Fig. 5. PCA analysis based on relative abundance SCCP homologues distribution after different oxidation treatment. Reaction conditions: 5 g of SCCPs contaminated soil (1 mg kg^{-1}), the water/soil ratio 1:1.5, initial pH 4.5 and ambient temperature.

3.3. Relationship between different homologues and oxidation modes

Table S2~S5 in the Supporting Information presented the abundance changes of different SCCP homologues after different oxidations. It was discovered that the abundance of some SCCP homologues increased, while others decreased, and the abundance changes followed a certain regularity: (i) SCCP homologues with a significant decrease in abundance included: $C_{10}Cl_{5\sim7}$, $C_{11}Cl_{5\sim7}$, and $C_{12}Cl_{6\sim7}$, while those homologues with a significant increase in abundance included: $C_{10}Cl_{8\sim10}$, $C_{11}Cl_{8\sim10}$, $C_{12}Cl_{8\sim10}$, and $C_{13}Cl_{8\sim10}$, which were significantly correlated with the number of chlorine atoms; (ii) There was the greatest decrease in the abundance of $C_{11}H_{18}Cl_6$ among the SCCP homologues, which indicated that it might be the most susceptible to oxidize; (iii) The abundance of $C_{10}H_{13}Cl_9$ increased the most, followed by $C_{13}H_{20}Cl_8$, proving that they might be very difficult to oxidize, or those longer chain CPs were mainly degraded into these two SCCPs after

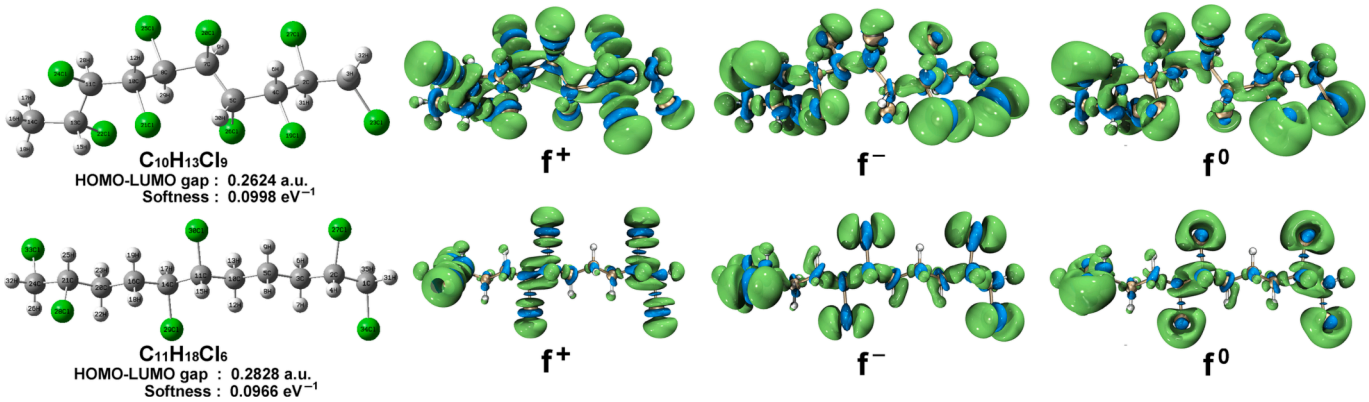

Fig. 6. The specific structures of $C_{11}H_{18}Cl_6$ and $C_{10}H_{13}Cl_9$ by DFT theoretical calculation (The green and blue colors represent the positive and negative phases of the molecular orbital). (For interpretation of the references to colour in this figure legend, the reader is referred to the web version of this article.)

oxidation.

In order to better analyze these phenomena and explore the degradation mechanism of SCCPs, we further confirmed the specific structures of $C_{11}H_{18}Cl_6$ and $C_{10}H_{13}Cl_9$ by DFT theoretical calculation. The highest occupied molecular orbital (HOMO)-lowest unoccupied molecular orbital (LUMO) energy separation (HOMO-LUMO gap) and chemical softness of molecules were calculated. Moreover, the Fukui Function was used to analyze the vulnerable sites of SCCPs. The HOMO-LUMO gap has been used as an indicator of kinetic stability. In general, a smaller HOMO-LUMO gap implies lower kinetic stability and higher chemical reactivity, since it is energetically advantageous to add electrons to LUMO at high position, or to extract electrons from HOMO at low position [38,39]. The degree of softness reflects the activity of electrons and the deformability of their distribution. In congeners, it is generally believed that the greater the softness, the more likely the molecule is to react [40,41]. Compared to $C_{11}H_{18}Cl_6$, $C_{10}H_{13}Cl_9$ had lower HOMO-LUMO gap and greater softness, which indicated that it was more easily oxidized, even though it possessed more chlorine atoms. The results indicated that the reason for the most increase in $C_{10}H_{13}Cl_9$ content was that those longer chain CPs were mainly degraded to $C_{10}H_{13}Cl_9$ after oxidation, rather than that it was more difficult to oxidize. In addition, the isosurface of Fukui index was presented in the Supporting Information, Tables S6~S7. The values of f^+, f^-, and f^0 represented nucleophilic attack, electrophilic attack, and radical attack

Table 2
The abundance changes of the SCCP homologue profiles classified by carbon and chlorine atomic number (blue and orange represented the relative abundance of SCCPs increased and decreased, respectively).

H	C_{10}	C_{11}	C_{12}	C_{13}	Cl_5	Cl_6	Cl_7	Cl_8	Cl_9	Cl_{10}
H1	1.22%	-3.66%	-0.44%	2.88%	0.22%	-8.94%	-4.09%	3.65%	5.01%	4.15%
H2	0.65%	-4.78%	-0.13%	4.25%	0.02%	-9.75%	-4.72%	4.28%	5.45%	4.71%
H3	-0.26%	-4.56%	0.45%	4.37%	-0.32%	-10.06%	-4.07%	4.32%	5.61%	4.51%
H4	0.04%	-4.58%	0.71%	3.83%	-0.15%	-9.99%	-3.95%	4.31%	5.23%	4.56%
F	C_{10}	C_{11}	C_{12}	C_{13}	Cl_5	Cl_6	Cl_7	Cl_8	Cl_9	Cl_{10}
F1	-0.14%	-4.25%	0.10%	4.29%	-1.20%	-10.84%	-3.77%	5.18%	5.75%	4.89%
F2	-2.23%	-4.69%	1.11%	5.81%	-1.73%	-12.56%	-3.38%	6.18%	6.61%	4.88%
F3	-1.58%	-4.98%	0.79%	5.77%	-1.64%	-12.33%	-3.84%	6.06%	6.38%	5.38%
F4	-2.52%	-5.34%	1.44%	6.43%	-1.91%	-13.14%	-3.36%	6.78%	6.68%	4.95%
P	C_{10}	C_{11}	C_{12}	C_{13}	Cl_5	Cl_6	Cl_7	Cl_8	Cl_9	Cl_{10}
P1	0.80%	-3.84%	0.15%	2.89%	-0.85%	-9.47%	-3.38%	4.36%	5.08%	4.26%
P2	0.405%	-3.90%	-0.10%	3.60%	-0.81%	-9.92%	-3.86%	4.28%	5.56%	4.76%
P3	1.46%	-3.18%	-0.89%	2.57%	-0.49%	-9.28%	-4.04%	3.72%	5.29%	4.79%
P4	2.10%	-3.07%	-0.70%	1.66%	-0.29%	-7.56%	-2.41%	3.49%	3.78%	2.99%
K	C_{10}	C_{11}	C_{12}	C_{13}	Cl_5	Cl_6	Cl_7	Cl_8	Cl_9	Cl_{10}
K1	0.72%	-3.65%	-0.38%	3.31%	-1.12%	-10.34%	-3.21%	4.63%	5.37%	4.67%
K2	-0.03%	-4.20%	0.13%	4.09%	-1.23%	-10.99%	-3.32%	5.15%	5.67%	4.71%
K3	-0.22%	-3.75%	0.19%	3.78%	-1.35%	-10.87%	-3.19%	5.39%	5.35%	4.66%
K4	0.12%	-4.27%	0.16%	3.99%	-1.56%	-11.25%	-2.97%	5.40%	5.70%	4.67%

respectively. In general, the higher Fukui index level, the more vulnerable site to attack [42]. It could be seen that the Fukui index level (f^+, f^-, and f^0) of chlorine atoms was the highest in both SCCP congeners, indicating that they were priority sites for attack during the oxidation process.

Furthermore, the SCCP homologue profiles were categorized and analyzed by carbon and chlorine atomic number, as shown in Table 2. For example, C_{11} consisted of $C_{11}H_{19}Cl_5$ + $C_{11}H_{18}Cl_6$ + $C_{11}H_{17}Cl_7$ + $C_{11}H_{16}Cl_8$ + $C_{11}H_{15}Cl_9$ + $C_{11}H_{14}Cl_{10}$, and so on. It could be clearly seen that there was a significant correlation between the number of carbon/chlorine atoms and the degradation result, especially for chlorine atoms. Along the oxidation process, there was a significant decrease in the relative abundance of C_{11} homologues, showing that SCCPs with carbon atom number of 11 were the most easily degraded. No obvious variation of C_{12} homologues was found. The relative abundance of C_{13} homologues increased obviously, which indicated that SCCPs with carbon atom number of 13 were the most difficult to degrade. In general, the relative abundance of SCCPs with chlorine atom number 5 ~ 7 showed a decreasing trend, while the relative abundance of SCCPs with chlorine atom number 8 ~ 10 showed an obvious increasing trend. Moreover, it was generally believed that POPs with higher chlorinated content would be more difficultly degraded, but there was no absolute negative correlation from our observation results. For example, Cl_6 homologue profiles of SCCPs were easier to be degraded than those of Cl_5 homologue profiles, which could be related to the position of the chlorine atoms on the SCCPs. These results indicated that the actual oxidation process of SCCPs could be more complex.

3.4. Relationship between atomic percentage and degradation efficiency

To better understand the relationship between carbon content, chlorine content and degradation efficiency of SCCPs, correlation analysis of all degradation experiments (1152 samples) was carried out, as shown in Table S8. As expected, there was a significant negative correlation between the carbon/chlorine atomic percentage and the degradation efficiency of SCCPs in oxidation process ($P < 0.01$). The negative correlation coefficient between the chlorine atomic percentage and the degradation efficiency was −0.439, which was significantly lower than that between the carbon atomic percentage and the degradation efficiency (−0.113), further confirming that the greater impact of the chlorine atomic percentage on the degradation of SCCPs.

In order to further explore the relationship between atomic species, content and degradation efficiency of SCCPs, chlorine atomic percentage and degradation efficiency in different treatments were plotted and analyzed. The result of the treatment with 2 % oxidants was representative, which was selected for analysis (Fig. 7), while the results of the others were also shown in the Supporting Information, Fig. S2. A significant negative correlation could be clearly observed between chlorine atomic mass percentage and the degradation efficiency of SCCPs, indicating the presence of chlorine atoms made SCCPs more difficult to degrade. Interestingly, four congeners consistently failed to follow this pattern, including $C_{12}H_{21}Cl_5$, $C_{13}H_{22}Cl_6$, $C_{12}H_{16}Cl_{10}$, and $C_{13}H_{18}Cl_{10}$. It was explained that the different position of chlorine atoms would affect the structural stability, which might lead to irregularity in the statistics according to the molecular formula. Excluding these homologues, good linear relationships and significant negative correlations were presented ($P < 0.01$).

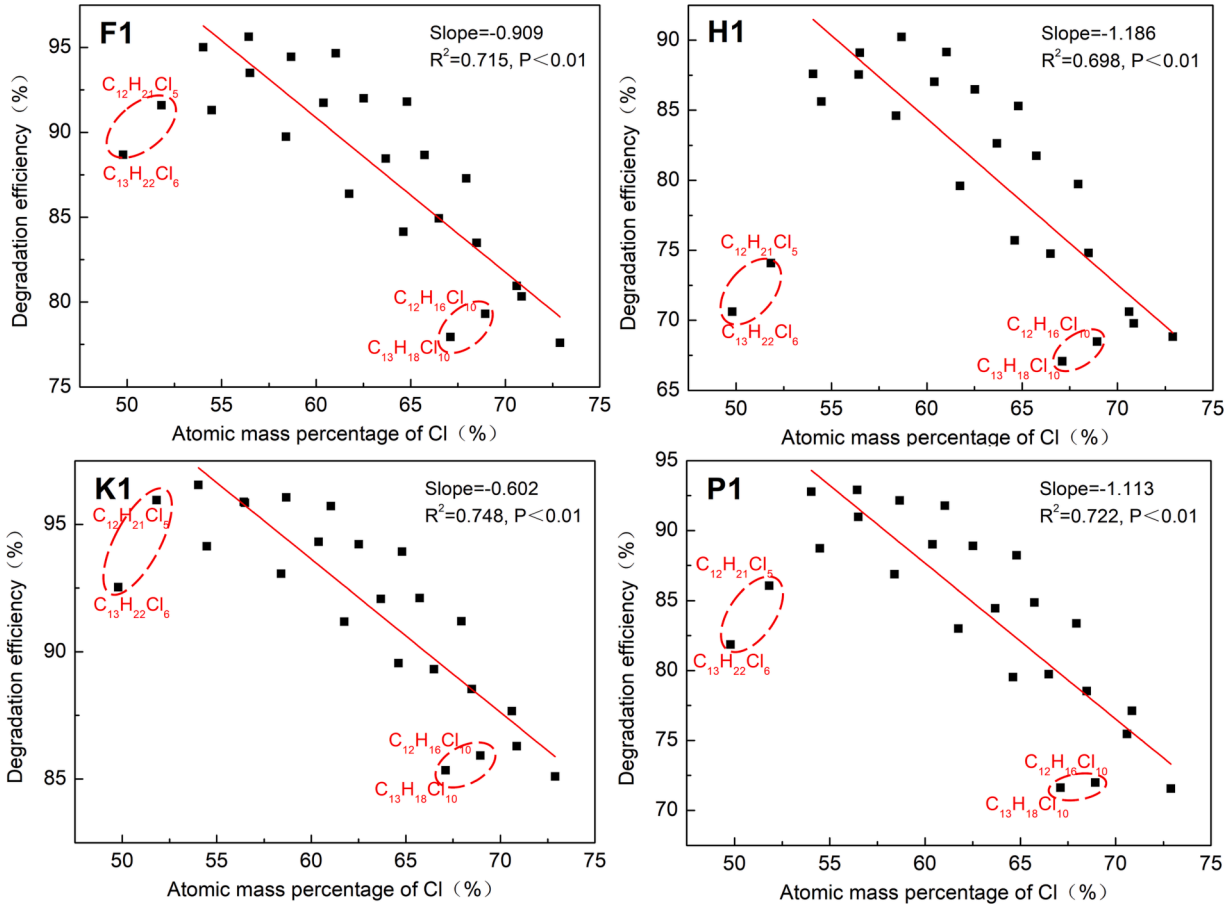

Fig. 7. The chlorine atomic percentage and degradation efficiency in different treatment conditions. Reaction conditions: 5 g of SCCPs contaminated soil (1 mg kg^{-1}), the water/soil ratio 1:1.5, initial pH 4.5 and ambient temperature.

4. Conclusions

Although there has been widespread concern about SCCPs pollution, the oxidation behavior of these compounds in contaminated soil still remains unknown. Herein, we systemically investigated the behavior and fate of SCCPs in four different reaction systems, including H_2O_2, Fenton, $KMnO_4$, and $Na_2S_2O_8$ treatment. The results revealed that ∑SCCPs decreased significantly within 120 h, and the order of the degradation efficiency under the optimal dosage conditions was followed as $KMnO_4$ > $Na_2S_2O_8$ > Fenton > H_2O_2. The degradation efficiency of SCCPs did not always increase with the increasing oxidant amount, and oxidants with too good oxidizing capacity might even lead to a rise in some SCCP congeners. Significant differences in SCCP homologue profiles were seen after oxidation treatment, among which the homologues with a significant decrease in abundance included: $C_{10}Cl_{5\sim7}$, $C_{11}Cl_{5\sim7}$, and $C_{12}Cl_{6\sim7}$, while those homologues with a significant increase in abundance included: $C_{10}Cl_{8\sim10}$, $C_{11}Cl_{8\sim10}$, $C_{12}Cl_{8\sim10}$, and $C_{13}Cl_{8\sim10}$. It was worth noting that among SCCP homologues, $C_{11}H_{18}Cl_6$ had the greatest decrease in abundance, while $C_{10}H_{13}Cl_9$ had the most increase in abundance, followed by $C_{13}H_{20}Cl_8$. DFT calculations indirectly proved that the most increase of $C_{10}H_{13}Cl_9$ was due to the major degradation of longer chain CPs to $C_{10}H_{13}Cl_9$ after oxidation. The chlorine atomic percentage had a greater impact on the degradation of SCCPs and there was a significant negative correlation between chlorine atomic percentage and degradation efficiency of SCCPs, only four congeners ($C_{12}H_{21}Cl_5$, $C_{13}H_{22}Cl_6$, $C_{12}H_{16}Cl_{10}$, and $C_{13}H_{18}Cl_{10}$) consistently failed to follow this pattern. The behavior and fate of SCCPs in different oxidation reactions were very complex, as the degradation degree was highly related to the atomic ratio and homologues composition, thus, the actual site restoration should comprehensively consider the types of pollutants, amount of oxidant, price, soil pH, and other conditions to select the appropriate oxidation methods. Our results provide insight into the behavior and fate of SCCPs in common oxidant reactions and data support for the actual SCCPs contaminated site remediation.

Declaration of Competing Interest

The authors declare that they have no known competing financial interests or personal relationships that could have appeared to influence the work reported in this paper.

Data availability

The authors do not have permission to share data.

Acknowledgements

The study was financially supported by the National Key R&D Program of China (No. 2019YFC1803900) and Guangzhou Science and Technology Plan (No. 202102080441).

Appendix A. Supplementary data

Supplementary data to this article can be found online at https://doi.org/10.1016/j.cej.2023.142557.

References

[1] M. Wang, Y. Gao, G. Li, T. An, Increased adverse effects during metabolic transformation of short-chain chlorinated paraffins by cytochrome P450: A theoretical insight into 1-chlorodecane, J. Hazard. Mater. 407 (2021), 124391, https://doi.org/10.1016/j.jhazmat.2020.124391.
[2] S. Bayen, J.P. Obbard, G.O. Thomas, Chlorinated paraffins: A review of analysis and environmental occurrence, Environ. Int. 32 (2006) 915–929, https://doi.org/10.1016/j.envint.2006.05.009.
[3] F.J. Santos, J. Parera, M.T. Galceran, Analysis of polychlorinated n-alkanes in environmental samples, Anal. Bioanal. Chem. 386 (2006) 837–857, https://doi.org/10.1007/s00216-006-0685-x.
[4] X. Du, B. Yuan, Y. Zhou, Z. Zheng, Y. Wu, Y. Qiu, J. Zhao, G. Yin, Tissue-Specific Accumulation, Sexual Difference, and Maternal Transfer of Chlorinated Paraffins in Black-Spotted Frogs, Environ. Sci. Technol. 53 (2019) 4739–4746, https://doi.org/10.1021/acs.est.8b06350.
[5] S. Endo, J. Hammer, Predicting Partition Coefficients of Short-Chain Chlorinated Paraffin Congeners by COSMO-RS-Trained Fragment Contribution Models, Environ. Sci. Technol. 54 (2020) 15162–15169, https://doi.org/10.1021/acs.est.0c06506.
[6] W. Vetter, J. Sprengel, K. Krätschmer, Chlorinated paraffins – A historical consideration including remarks on their complexity, Chemosphere. 287 (2022), 132032, https://doi.org/10.1016/j.chemosphere.2021.132032.
[7] Poprc, The New POPs under the Stockholm Convention, Geneva. Available at: Persistent Organic Pollutants Review Committee. (2017) http://chm.pops.int/ TheConvention/ThePOPs/TheNewPOPs/tabid/2511/Default.aspx.,.
[8] C. Chen, A. Chen, L. Li, W. Peng, R. Weber, J. Liu, Distribution and Emission Estimation of Short- And Medium-Chain Chlorinated Paraffins in Chinese Products through Detection-Based Mass Balancing, Environ. Sci. Technol. 55 (2021) 7335–7343, https://doi.org/10.1021/acs.est.0c07058.
[9] W. Wang, J. Wang, H. Nie, R. Fan, Y. Huang, Occurrence, trophic magnification and potential risk of short-chain chlorinated paraffins in coral reef fish from the Nansha Islands, South China Sea, Sci. Total Environ. 739 (2020), 140084, https://doi.org/10.1016/j.scitotenv.2020.140084.
[10] Y. Guida, R. Capella, N. Kajiwara, J.O. Babayemi, J.P.M. Torres, R. Weber, Inventory approach for short-chain chlorinated paraffins for the Stockholm Convention implementation in Brazil, Chemosphere. 287 (2022), 132344, https://doi.org/10.1016/j.chemosphere.2021.132344.
[11] B. Yuan, D. Muir, M. MacLeod, Methods for trace analysis of short-, medium-, and long-chain chlorinated paraffins: Critical review and recommendations, Anal. Chim. Acta. 1074 (2019) 16–32, https://doi.org/10.1016/j.aca.2019.02.051.
[12] X. Wang, J. Zhu, Z. Xue, X. Jin, Y. Jin, Z. Fu, The environmental distribution and toxicity of short-chain chlorinated paraffins and underlying mechanisms: Implications for further toxicological investigation, Sci. Total Environ. 695 (2019), 133834, https://doi.org/10.1016/j.scitotenv.2019.133834.
[13] G.L. Wei, X.L. Liang, D.Q. Li, M.N. Zhuo, S.Y. Zhang, Q.X. Huang, Y.S. Liao, Z. Y. Xie, T.L. Guo, Z.J. Yuan, Occurrence, fate and ecological risk of chlorinated paraffins in Asia: A review, Environ. Int. 92–93 (2016) 373–387, https://doi.org/10.1016/j.envint.2016.04.002.
[14] K. Vorkamp, J. Balmer, H. Hung, R.J. Letcher, F.F. Rigét, A review of chlorinated paraffin contamination in Arctic ecosystems, Emerg. Contam. 5 (2019) 219–231, https://doi.org/10.1016/j.emcon.2019.06.001.
[15] W. Jiang, T. Huang, H. Chen, L. Lian, X. Liang, C. Jia, H. Gao, X. Mao, Y. Zhao, J. Ma, Contamination of short-chain chlorinated paraffins to the biotic and abiotic environments in the Bohai Sea, Environ. Pollut. 233 (2018) 114–124, https://doi.org/10.1016/j.envpol.2017.10.034.
[16] M. Zhuo, S. Ma, G. Li, Y. Yu, T. An, Chlorinated paraffins in the indoor and outdoor atmospheric particles from the Pearl River Delta: Characteristics, sources, and human exposure risks, Sci. Total Environ. 650 (2019) 1041–1049, https://doi.org/10.1016/j.scitotenv.2018.09.107.
[17] Y. Wu, J. Wu, H. Tan, Q. Song, J. Zhang, X. Zhong, J. Zhou, W. Wu, X. Cai, W. Zhang, X. Liu, Distributions of chlorinated paraffins and the effects on soil microbial community structure in a production plant brownfield site, Environ. Pollut. 262 (2020), 114328, https://doi.org/10.1016/j.envpol.2020.114328.
[18] M.A. Oturan, J.J. Aaron, Advanced oxidation processes in water/wastewater treatment: Principles and applications. A review, Crit Rev, Environ. Sci. Technol. 44 (2014) 2577–2641, https://doi.org/10.1080/10643389.2013.829765.
[19] M. Vallejo, M. Fresnedo San Román, I. Ortiz, A. Irabien, Overview of the PCDD/Fs degradation potential and formation risk in the application of advanced oxidation processes (AOPs) to wastewater treatment, Chemosphere. 118 (2015) 44–56.
[20] J. Wang, S. Wang, Reactive species in advanced oxidation processes: Formation, identification and reaction mechanism, Chem. Eng. J. 401 (2020), 126158, https://doi.org/10.1016/j.cej.2020.126158.
[21] Y. Li, H. Dong, L. Li, L. Tang, R. Tian, R. Li, J. Chen, Q. Xie, Z. Jin, J. Xiao, S. Xiao, G. Zeng, Recent advances in waste water treatment through transition metal sulfides-based advanced oxidation processes, Water Res. 192 (2021), 116850, https://doi.org/10.1016/j.watres.2021.116850.
[22] W. Zhang, Y. Gao, Y. Qin, M. Wang, J. Wu, G. Li, T. An, Photochemical degradation kinetics and mechanism of short-chain chlorinated paraffins in aqueous solution: A case of 1-chlorodecane, Environ. Pollut. 247 (2019) 362–370, https://doi.org/10.1016/j.envpol.2019.01.065.
[23] J. Schönherr, J. Buchheim, P. Scholz, M. Stelter, Oxidation of carbon nanotubes with ozone and hydroxyl radicals, Carbon. 111 (2017) 631–640, https://doi.org/10.1016/j.carbon.2016.10.013.
[24] R.G. Parr, W. Yang, Theory of Orientation and Steroselection, Springer-Verlag, 1984 https://pubs.acs.org/sharingguidelines.
[25] C. Morell, A. Grand, A. Toro-Labbé, New dual descriptor for chemical reactivity, J. Phys. Chem. A. 109 (2005) 205–212, https://doi.org/10.1021/jp046577a.
[26] T. Lu, F. Chen, Multiwfn: A multifunctional wavefunction analyzer, J. Comput. Chem. 33 (2012) 580–592, https://doi.org/10.1002/jcc.22885.
[27] R. Fu, T. Lu, F.W. Chen, Comparing methods for predicting the reactive site of electrophilic substitution, Wuli Huaxue Xuebao/ Acta Physico - Chimica Sinica. 30 (2014) 628–639, https://doi.org/10.3866/PKU.WHXB201401211.
[28] X. Pan, J. Wei, M. Zou, J. Chen, R. Qu, Z. Wang, Products distribution and contribution of (de)chlorination, hydroxylation and coupling reactions to 2,4-

dichlorophenol removal in seven oxidation systems, Water Res. 194 (2021), 116916, https://doi.org/10.1016/j.watres.2021.116916.
[29] C. Ma, X. Huangfu, Y. Zou, R. Huang, Q. He, J. Ma, Kinetics and mechanism of Thallium(I) oxidation by Permanganate: Role of bromide, Chemosphere. 293 (2022), 133652, https://doi.org/10.1016/j.chemosphere.2022.133652.
[30] J. Peng, P. Zhou, H. Zhou, W. Liu, H. Zhang, C. Zhou, L. Lai, Z. Ao, S. Su, B. Lai, Insights into the Electron-Transfer Mechanism of Permanganate Activation by Graphite for Enhanced Oxidation of Sulfamethoxazole, Environ. Sci. Technol. 55 (2021) 9189–9198, https://doi.org/10.1021/acs.est.1c00020.
[31] J. Li, S.Y. Pang, Z. Wang, Q. Guo, J. Duan, S. Sun, L. Wang, Y. Cao, J. Jiang, Oxidative transformation of emerging organic contaminants by aqueous permanganate: Kinetics, products, toxicity changes, and effects of manganese products, Water Res. 203 (2021), 117513, https://doi.org/10.1016/j.watres.2021.117513.
[32] Z. Zhou, X. Liu, K. Sun, C. Lin, J. Ma, M. He, W. Ouyang, Persulfate-based advanced oxidation processes (AOPs) for organic-contaminated soil remediation: A review, Chem. Eng. J. 372 (2019) 836–851, https://doi.org/10.1016/j.cej.2019.04.213.
[33] Z. Han, S. Li, Y. Yue, Y. Tian, S. Wang, Z. Qin, L. Ji, D. Han, W. Jiao, Enhancing remediation of PAH-contaminated soil through coupling electrical resistance heating using $Na_2S_2O_8$, Environ. Res. 198 (2021), 110457, https://doi.org/10.1016/j.envres.2020.110457.
[34] M. Usman, K. Hanna, P. Faure, Remediation of oil-contaminated harbor sediments by chemical oxidation, Sci. Total Environ. 634 (2018) 1100–1107, https://doi.org/10.1016/j.scitotenv.2018.04.092.
[35] Y. Liu, Y. Zhao, J. Wang, Fenton/Fenton-like processes with in-situ production of hydrogen peroxide/hydroxyl radical for degradation of emerging contaminants: Advances and prospects, J. Hazard. Mater. 404 (2021), 124191, https://doi.org/10.1016/j.jhazmat.2020.124191.
[36] A. Babuponnusami, K. Muthukumar, Advanced oxidation of phenol: A comparison between Fenton, electro-Fenton, sono-electro-Fenton and photo-electro-Fenton processes, Chem. Eng. J. 183 (2012) 1–9, https://doi.org/10.1016/j.cej.2011.12.010.
[37] O.S. Keen, S. Baik, K.G. Linden, D.S. Aga, N.G. Love, Enhanced biodegradation of carbamazepine after UV/H_2O_2 advanced oxidation, Environ. Sci. Technol. 46 (2012) 6222–6227, https://doi.org/10.1021/es300897u.
[38] J.I. Aihara, Reduced HOMO-LUMO Gap as an Index of Kinetic Stability for Polycyclic Aromatic Hydrocarbons, J. Phys. Chem. A. 103 (1999) 7487–7495, https://doi.org/10.1021/jp990092i.
[39] D.F. Perepichka, M.R. Bryce, Molecules with exceptionally small HOMO-LUMO gaps, Angew. Chem. - Int. Edit. 44 (2005) 5370–5373, https://doi.org/10.1002/anie.200500413.
[40] R.G. Pearson, Chemical hardness and density functional theory, J Chem Sci 117 (5) (2005) 369–377.
[41] S. Saha, T.C. Dinadayalane, D. Leszczynska, J. Leszczynski, Open and capped (5,5) armchair SWCNTs: A comparative study of DFT-based reactivity descriptors, Chem. Phys. Lett. 541 (2012) 85–91, https://doi.org/10.1016/j.cplett.2012.05.050.
[42] C. Zhang, S. Tian, F. Qin, Y. Yu, D. Huang, A. Duan, C. Zhou, Y. Yang, W. Wang, Y. Zhou, H. Luo, Catalyst-free activation of permanganate under visible light irradiation for sulfamethazine degradation: Experiments and theoretical calculation, Water Res. 194 (2021), 116915, https://doi.org/10.1016/j.watres.2021.116915.